NUCLEAR INSTRUMENTS AND METHODS 66 (1968) 61–69; © NORTH-HOLLAND PUBLISHING CO.

DIRECTIONAL-CORRELATION ATTENUATION FACTORS FOR Ge(Li) γ-RAY DETECTORS*

W. G. WINN and D. G. SARANTITES

Department of Chemistry, Washington University, St. Louis, Missouri, U.S.A.

Received 9 July 1968

An experimental method for the determination of the angular correlation attenuation factors, due to finite solid angle, for Ge(Li) detectors is offered. The method is tested by comparing the measured factors for a 3″ × 3″ NaI(Tl) detector with available calculated attenuation factors. Results for two coaxial Ge(Li) detectors with active volumes of 20 and 30 cm^3 are presented as a function of distance and energy of the γ-rays. These correction factors were further tested by comparison of the results of measurements of an angular correlation from a ^{207}Bi source, with previously reported results.

Of considerable interest is the application of high resolution Ge(Li) γ-ray detectors in measurements of angular correlations between coincident γ-rays. Hindrances in such measurements, other than the low detection efficiency of Ge(Li) detectors, arise from the fact that the corrections for the attenuation of the angular correlations due to the finite solid angle are difficult to evaluate. This is particularly true here, as the exact shape and size of the sensitive volume of the Ge(Li) detectors is not known, and one has to rely on the manufacturer's "guess" for the precise drift depth and the uniformity of the intrinsic layer. In this note we present an experimental method for measuring the correction factors which does not require the exact knowledge of the detector shape.

Usually an experimental directional correlation measured with two cylindrical detectors A and B which detect γ rays γ_1 and γ_2, respectively, is written as[1])

$$W_{\exp}(\theta)/A_0 = 1 + Q_2^{\mathrm{A}}(\gamma_1)Q_2^{\mathrm{B}}(\gamma_2)A_{22}P_2(\cos\theta) + Q_4^{\mathrm{A}}(\gamma_1)Q_4^{\mathrm{B}}(\gamma_2)A_{44}P_4(\cos\theta), \quad (1)$$

where Q_{2n}^{A} and Q_{2n}^{B} are the attenuation factors at the energies of γ_1 and γ_2, A_{22} and A_{44} are the directional correlation coefficients which depend on the spins of the nuclear levels connected by the cascade, and $P_2(\cos\theta)$ and $P_4(\cos\theta)$ are the second and fourth Legendre polynomials, respectively.

For each detector and γ-ray energy, Q_{2n} is given by[1,2])

$$Q_{2n} = \int_0^{\alpha} \varepsilon(\beta)P_{2n}(\cos\beta)\mathrm{d}(\cos\beta) \Big/ \int_0^{\alpha} \varepsilon(\beta)\mathrm{d}(\cos\beta), \quad (2)$$

where $\varepsilon(\beta)$ is the full-energy peak efficiency of the detector for the energy in question, when the incident γ ray forms an angle β with the symmetry axis of the detector, and α is the maximum value of β (fig. 1A). Writing $P_{2n}(\cos\beta)$ in the usual form of polynomials in $\cos\beta$, and substituting into eq. (2), yields

$$Q_2 = \tfrac{3}{2}R_2 - \tfrac{1}{2}, \quad (3)$$

$$Q_4 = \tfrac{35}{8}R_4 - \tfrac{30}{8}R_2 + \tfrac{3}{8}, \quad (4)$$

where

$$R_{2n} = \int_0^{\alpha} \varepsilon(\beta)\cos^{2n}\beta\,\mathrm{d}(\cos\beta) \Big/ \int_0^{\alpha} \varepsilon(\beta)\mathrm{d}(\cos\beta). \quad (5)$$

The denominator in eq. (5) is the detection efficiency, at the full-energy peak, for the γ ray in question, while the numerator is smaller than this efficiency because $0 \leqq \cos^{2n}\beta \leqq 1$. Imagining the $\cos^{2n}\beta$ in eq. (5) as a γ-ray flux attenuator, we can design an absorber of thickness $t(\beta)$ such that

$$\exp\{-\mu t(\beta)\} = \cos^{2n}\beta, \quad (6)$$

or

$$t(\beta) = (2n/\mu)\ln\sec\beta, \quad (7)$$

where μ is the linear attenuation coefficient of the γ ray in the absorber. Using this absorber, one can evaluate R_{2n} of eq. (5) by counting the source with and without the absorber for equal time; the count ratio of the former to the latter is R_{2n}. The exact functional form of eq. (7) for the absorber thickness is such that it is difficult to machine. However, expanding $\ln\sec\beta$ in power series yields

$$t(\beta) = (2n/\mu)[(\sec\beta - 1) - \tfrac{1}{2}(\sec\beta - 1)^2 + \tfrac{1}{3}(\sec\beta - 1)^3 - \ldots]. \quad (8)$$

An absorber bounded by a plane tangent to a spherical surface of radius $r = 2n/\mu$ provides a thickness

$$t(\beta) = (2n/\mu)(\sec\beta - 1), \quad (9)$$

* This work was supported in part by the U.S. Atomic Energy Commission under Contract Nos. AT(11-1)-1530 and AT(11-1)-1760.

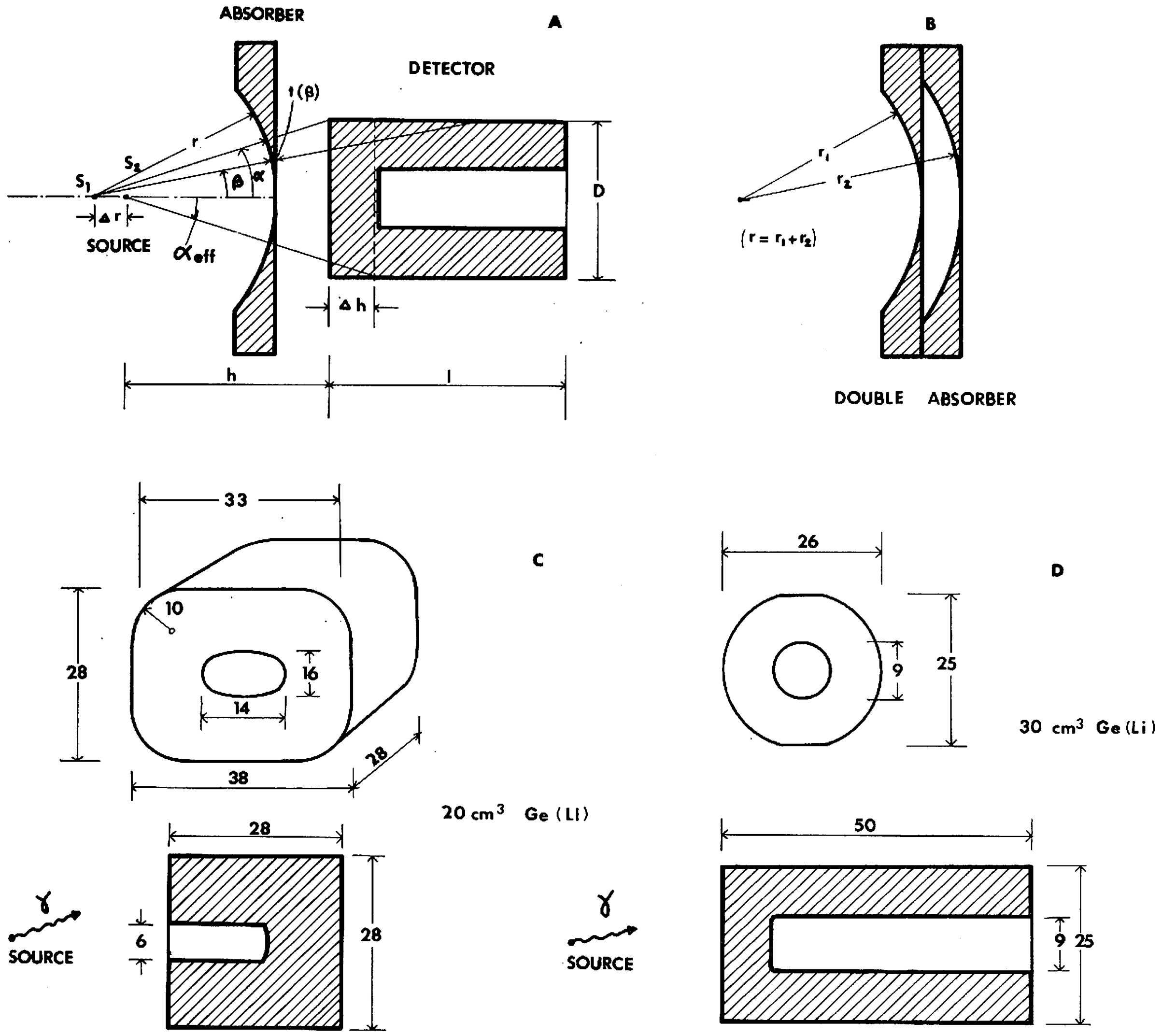

Fig. 1. A. Schematic representation of the source, absorber and detector for the measurement of Q_2 and Q_4.
B. Schematic representation of double absorbers used in some measurements of Q_2 and Q_4.
C. Dimensions of the rounded trapezoidal-type coaxial 20 cm³ Ge(Li) detector as provided by the manufacturer. All dimensions are given in mm.
D. Dimensions of the cylindrical coaxial 30 cm³ Ge(Li) detector. All dimensions are given in mm.

for a point source placed at the center of the spherical surface. This is a very good approximation to eq. (8) for $\beta \leqq 20°$. For extension to larger angles, moving the source by Δr from the center S_1 (fig. 1A) of the spherical surface toward the absorber modifies the form of eq. (9), allowing better agreement with eq. (8). In particular, we calculated that for a source at S_2 (fig. 1A), the thickness is given by

$$t(\beta) = (2n/\mu)\left[(\sec\beta - 1) - p\tan\beta\sin\beta + p^2\sin^2\beta/\{1+(1-p^2\sin^2\beta)^{\frac{1}{2}}\}\right], \quad (10)$$

where p is $\Delta r/r$. This expression reduces to eq. (9) for p equal to zero. For certain characteristic value p_0 of p, eq. (10) gives the same R_{2n} values as eq. (7). As the dependence of $t(\beta)$ on p_0 is of second order, a perturbation technique was applied for a suitable estimate. By requiring that

$$\int_0^{\alpha} \varepsilon(\beta)\cos^{2n}\beta \,\mathrm{d}(\cos\beta) = \int_0^{\alpha} \varepsilon(\beta)\exp\{-\mu t(\beta)\}\,\mathrm{d}(\cos\beta) \quad (11)$$

and setting $\varepsilon(\beta)$ equal to unity we obtained p_0. Here, for minimal error, p_0 should be evaluated for an effective angle α_{eff}, which describes the extension of the detector in this treatment. We define this effective angle in fig. 1A

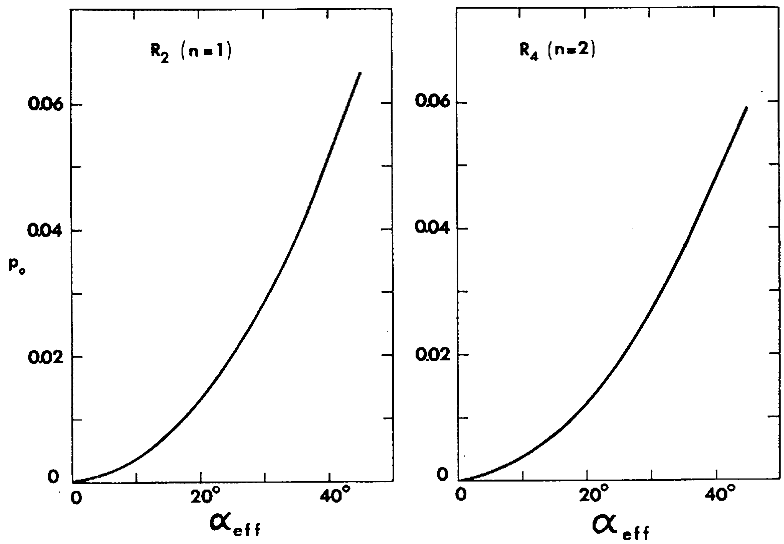

Fig. 2. Calculated values of p_0, giving the fractional displacement of the source toward the absorber for minimal error, as a function of α_{eff}.

by means of Δh, which to a useful approximation is given by

$$\Delta h(E_\gamma) = \mu_d^{-1}[1-\exp(-\tfrac{1}{2}l\mu_d)], \qquad (12)$$

where μ_d is the linear attenuation coefficient for the interaction of the γ ray in the detector. In fig. 2 we give the calculated values of p_0 as a function of α_{eff}.

In the present measurements we selected the following γ-ray sources: ^{139}Ce(166 keV), ^{203}Hg(279 keV), ^{113}Sn(393 keV), ^{54}Mn(835 keV) and ^{207}Bi (570 and 1064 keV). These sources either emit only one γ ray, or in the case of ^{207}Bi the γ rays are well apart in energy to permit accurate intensity measurements with the NaI(Tl) detectors. The choice of absorber material was made so that the resulting radius of the spherical surface was between 2.3 and 3.0 cm; the actual materials used were titanium, copper, iron and lead. The corresponding linear attenuation coefficients of the above γ rays were measured using a Ge(Li) detector with and without collimation; the resulting values of μ indicated that forward Compton scattering from the absorbers would not introduce noticeable errors. In some cases double absorbers had to be used in order to maintain the distance between source and absorber about 2.5 cm (fig. 1B). In table 1 we summarize the information on the design of the absorbers used.

We have tested this method by measuring Q_2 and Q_4 for a 3″ × 3″ NaI(Tl) detector, for which reliable calculations are available[2]). In fig. 3 we summarize the results of the measurement of Q_2 and Q_4 for a 3″ × 3″ NaI(Tl) detector, as a function of the source distance from the detector for the above mentioned γ ray energies. The solid curves have been drawn through the calculated points of Yates[2]). A detailed analysis of all possible sources of error was made and the results are discussed later. In general, the errors can be reduced by treating the data in the following manner. We have shown that to a very good approximation $R_4 = (1+\sigma)R_2^2$, where σ is almost independent of the energy of the γ ray and is quite small compared to unity ($\sigma < 0.005$ for $\alpha < 25°$). This allows one to combine the measured R_2 and R_4 values in calculating Q_2 and Q_4, and thus reduce the error. When this refinement was applied to the results for the 3″ × 3″ NaI(Tl) detector, the overall agreement between experimental and calculated values was improved, as shown in fig. 4.

TABLE 1

Absorber dimensions for measurment of Q_2 and Q_4.

E_γ (keV)	Material	$r=2/\mu$ (cm)	$r=4/\mu$ (cm)	Absorber	type
166	Ti	3.15	–	single	–
	Cu	–	2.53	–	single
279	Fe	2.35	–	single	–
	Fe	–	4.70	–	double
393	Cu	2.44	–	single	–
	Cu	–	4.88	–	double
570	Cu	2.96	–	single	–
	Pb	–	2.86	–	single
835	Pb	2.22	–	single	–
	Pb	–	4.44	–	double
1064	Pb	2.82	–	single	–
	Pb	–	5.64	–	double

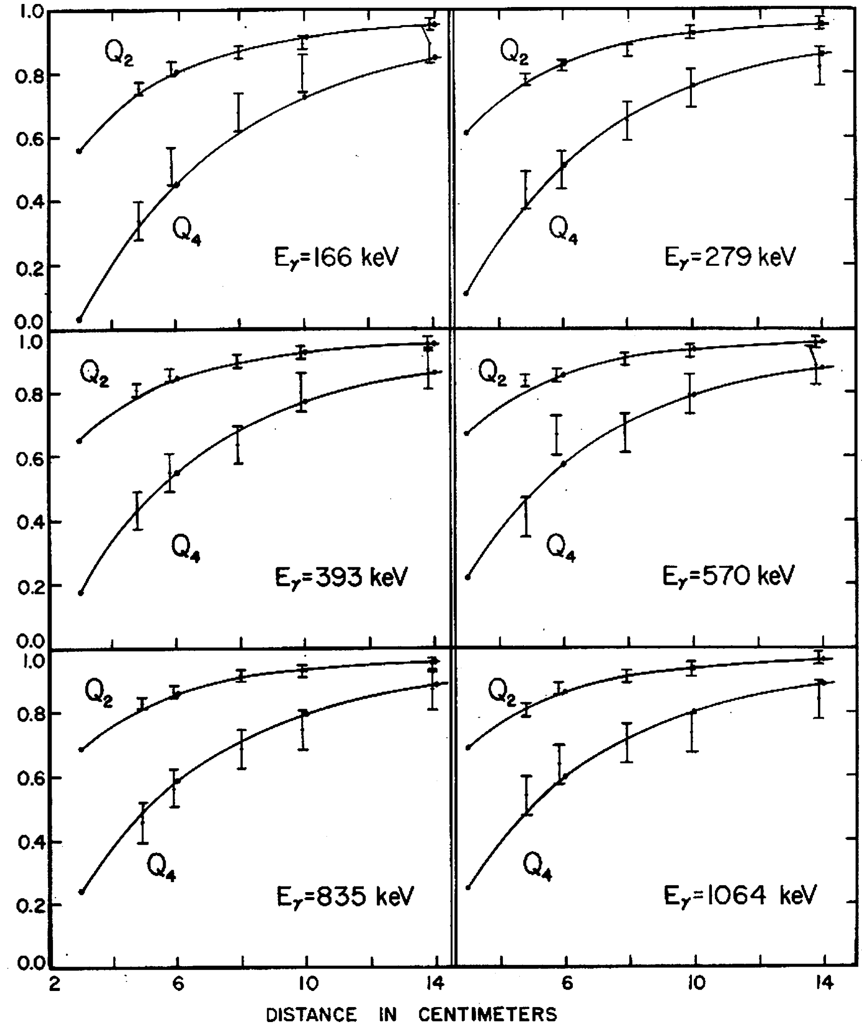

Fig. 3. Measured values for the directional-correlation attenuation factors Q_2 and Q_4 for a 3″ × 3″ NaI(Tl) detector. The solid lines are smooth lines drawn through the calculated values from [2]).

The two Ge(Li) detectors that were used for these measurements are of the coaxial type with 20 and 30 cm^3 nominal sensitive volumes. The dimensions provided by the manufacturer are shown in figs. 1c and d. Since the distance between detector and aluminum can is about 1 cm, in both cases, we have measured the correction factors at 3 cm from the can or 4 cm from the detectors, at the closest. In figs. 5 and 6 we show the results of the measurement of Q_2 and Q_4 as a function of energy for various distances, for the 30 and 20 cm^3 detectors, respectively. It should be emphasized here that these values refer to full-energy peak areas. A comparison of the general shapes of these curves for Ge(Li) detectors with the corresponding ones for NaI(Tl) detectors[2]) displays no obvious differences except for the higher energy (> 1 MeV) region, where the curves for Ge(Li) do not appear to level off as quickly as those for NaI(Tl) detectors.

Interpolation between distances or extrapolation to shorter distances distances (fig. 6, broken curve) can be adequately performed by means of the relation

$$\arccos R_2(\alpha) = a\alpha + b, \tag{13}$$

which was shown to be applicable to a good approximation for small ranges of angles, or ($10° \leqq \alpha \leqq 30°$) in the present measurements. We have, therefore, fitted the data points using this relation by the least-squares technique. The values from the best fit are shown as the data points in figs. 5 and 6. The values at 3 cm for the 20 cm^3 detector (fig. 6) were obtained by this functional extrapolation.

The intrinsic sources of error for this method applied to Ge(Li) detectors were analyzed in considerable detail. The results of this analysis for the worst anticipated case of each of the sources of error is summarized below. In table 2 we give the estimated percent error in R_2 and R_4 due to the fact that a small fraction of the forward Compton scattered γ rays in the absorber fall under the full energy peak. The values given in table 2 refer to a typical absorber radius of 25 mm, and were evaluated assuming that a 20% error for NaI(Tl) and 15% for Ge(Li) was made in the corresponding background under the full-energy peak. In table 3 we summarize the estimated errors in R_2 and R_4 due to uncertainties in the values of μ used (estimated to $\pm 2\%$ for these measurements) and to uncertainties in positioning the source at the point of optimum position S_2 (estimated to ± 0.1 mm for these measurements). These errors depend only on the solid angle and are tabulated as a function of α. It should be pointed out that for our Ge(Li) detectors the value of α at the closest distance used does not exceed 25°. Finally, in table 4 we summarize the errors in R_2 and R_4 due to extended sources, and for positioning the source off the symmetry axis of the detector and absorber. These errors are both negative and do not cancel by repeated measurements. A correction for extended sources can be applied to the measurements. The error in the radius in machining the spherical surface of the absorbers is included in errors in μ. A small correction for absorption due a thickness of 0.005 cm of absorber at its thinnest point was applied to all the data points. Errors due to uncertainties in tilting the absorber from its normal position (perpendicular to the detector axis) were shown to be negligible.

For the Ge(Li) detector, the overall estimated error of each individual measurement is less than 0.5% in R_2 and R_4. The estimated errors in Q_2 and Q_4 are 0.7%

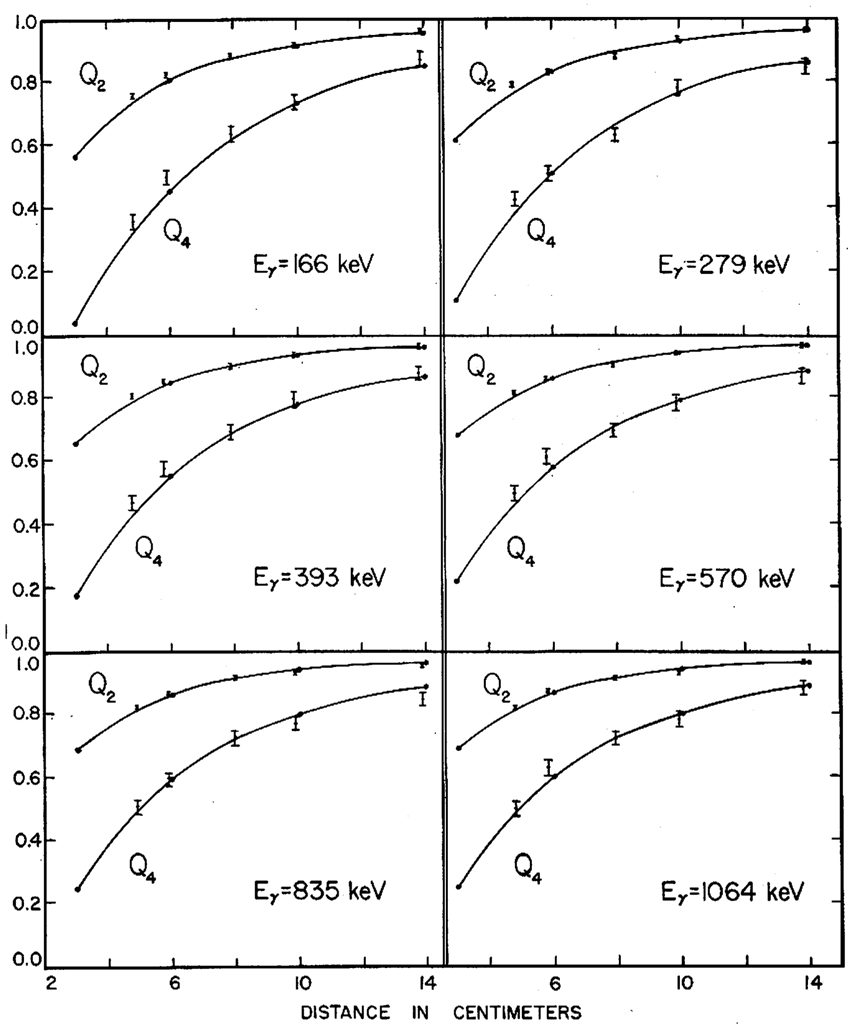

Fig. 4. Results of fig. 3 reanalyzed using the relation $R_4 = (1+\sigma)R_2^2$. The errors evaluated now are considerably smaller.

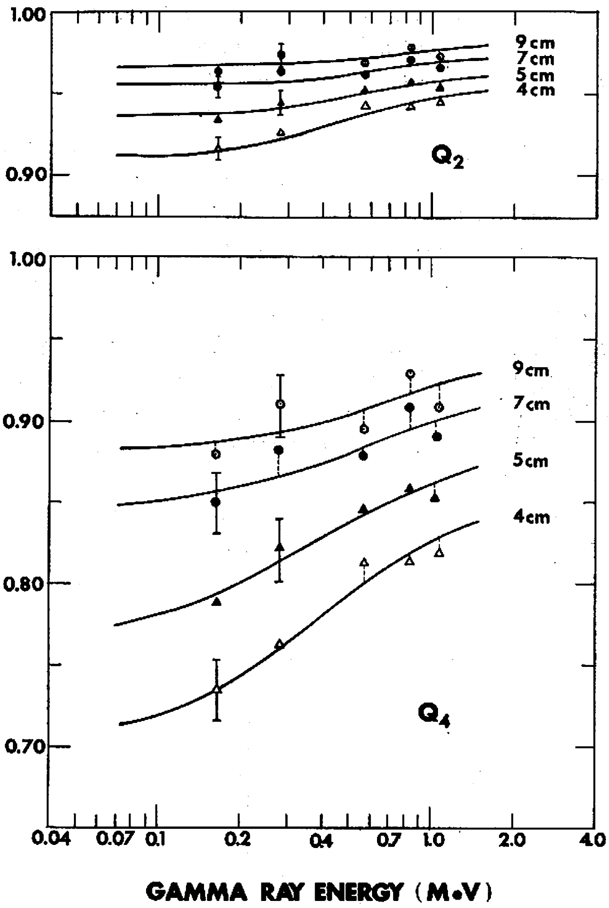

Fig. 5. Measured directional-correlation attenuation factors Q_2 and Q_4 for a cylindrical true coaxial 30 cm³ Ge(Li) detector. The distances are measured from the detector.

and 2.5%, respectively, when measurements of both R_2 and R_4 are taken, and use of the relation $R_4 = R_2^2(1+\sigma)$ is made in the calculation of Q_2 and Q_4. The overall estimated error in the curves fitted to the data points is $\leqq 0.5\%$ in Q_2 and $\leqq 1.5\%$ in Q_4.

Finally, use of one trapezoidal-type Ge(Li) detector with dimensions given in fig. 1c and another cylindrical detector, results in an angular distribution, the functional form of which deviates from that of eq. (1).

We have shown that for one trapezoidal and one cylindrical detector, eq. (1) can be written

$$W_{\exp}(\theta) = A_0[1 + A'_{22}F_2(\theta) + A'_{44}F_4(\theta)], \qquad (14)$$

with

$$A'_{22} = Q_2^{\mathrm{C}} Q_2^{\mathrm{T}} A_{22},$$

$$A'_{44} = Q_4^{\mathrm{C}} Q_4^{\mathrm{T}} A_{44},$$

where Q_2^{C} and Q_4^{C} refer to the cylindrical detector,

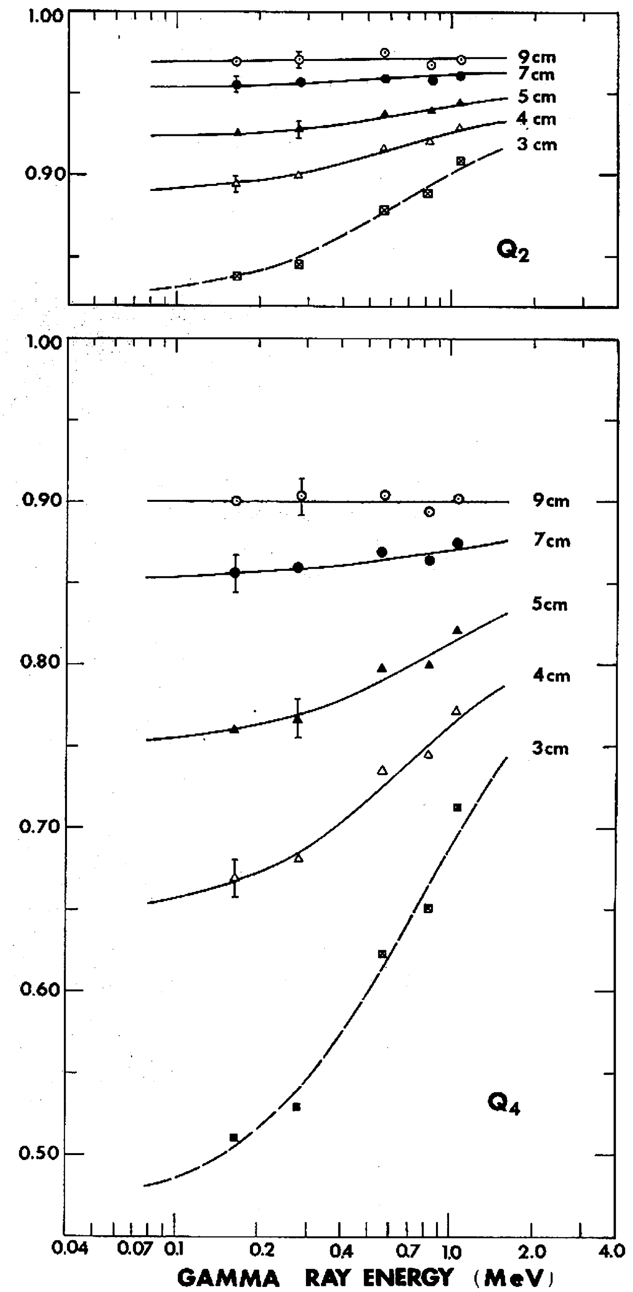

Fig. 6. Measured directional-correlation attenuation factors Q_2 and Q_4 for a near cylindrical coaxial 20 cm³ Ge(Li) detector. The values for the close distance (dashed curves) were obtained by proper functional extrapolation (see text). The distances are measured from the detector.

Q_2^{T} and Q_4^{T} refer to the trapezoidal detector, and $F_2(\theta)$ and $F_4(\theta)$ are given by*

$$F_2(\theta) = P_2(\cos\theta) + (C_{22}/Q_2^{\mathrm{T}})\sin^2\theta, \qquad (15)$$

$$F_4(\theta) = P_4(\cos\theta) + (C_{42}/Q_4^{\mathrm{T}})(7\cos^4\theta - 8\cos^2\theta + 1) + (C_{44}/Q_4^{\mathrm{T}})\sin^4\theta, \qquad (16)$$

* The $F(\theta)$'s correspond to the case where the symmetry plane of the trapezoidal detector is perpendicular to the θ-plane.

TABLE 2
Estimated % error in R_2 and R_4 due to forward Compton scattering under the full-energy peak.

E_γ(keV)	Absorber	NaI(Tl)	Ge(Li)
166	Ti	1.9	0.12
166	Cu	1.5	0.094
279	Fe	1.0	0.042
393	Cu	0.59	0.027
570	Cu	0.26	0.0096
570	Pb	0.14	0.0052
835	Pb	0.14	0.0040
1064	Pb	0.14	0.0036

where

$$C_{22} = -\frac{3}{4}\int_\Omega \varepsilon^{\mathrm{T}}(\beta,\gamma)\sin^2\beta\cos 2\gamma\,\mathrm{d}\Omega \Big/ \int_\Omega \varepsilon^{\mathrm{T}}(\beta,\gamma)\,\mathrm{d}\Omega, \quad (17)$$

$$C_{42} = -\frac{5}{16}\int_\Omega \varepsilon^{\mathrm{T}}(\beta,\gamma)(7\cos^4\beta - 8\cos^2\beta + 1)\cdot \cdot\cos 2\gamma\,\mathrm{d}\Omega \Big/ \int_\Omega \varepsilon^{\mathrm{T}}(\beta,\gamma)\,\mathrm{d}\Omega, \quad (18)$$

$$C_{44} = \frac{35}{64}\int_\Omega \varepsilon^{\mathrm{T}}(\beta,\gamma)\sin^4\beta\cos 4\gamma\,\mathrm{d}\Omega \Big/ \int_\Omega \varepsilon^{\mathrm{T}}(\beta,\gamma)\,\mathrm{d}\Omega, \quad (19)$$

and γ is the angle about the detector axis.

Approximate calculations using a "black" detector indicate that the values of C_{ij} are less than 0.1, for the closest distance used, thus representing less than 10% deviation of $F_{2n}(\theta)$ from $P_{2n}(\cos\theta)$. We have further shown that to a good approximation

$$C_{42} \cong -\tfrac{5}{2}C_{22} \text{ and } C_{44} \cong 0. \quad (20)$$

With this approximation eq. (14) becomes

$$W_{\exp}(\theta) = A_0\{1 + A'_{22}[P_2(\cos\theta) + \tfrac{3}{4}(X/Q_2^{\mathrm{T}})\sin^2\theta] + + A'_{44}[P_4(\cos\theta) - \tfrac{15}{8}(X/Q_4^{\mathrm{T}})(7\cos^4\theta - 8\cos^2\theta + 1)]\}, \quad (21)$$

TABLE 3
Estimated % errors in R_2 and R_4 due to uncertainties in μ and in positioning of the source along symmetry axis.

α	% error for 1% error in μ		% error for 0.1 mm error in positioning the source	
	R_2	R_4	R_2	R_4
0°	0	0	0	0
10°	±0.03	±0.056	±0.032	±0.052
20°	±0.062	±0.12	±0.068	±0.14
30°	±0.14	±0.25	±0.14	±0.26
40°	±0.23	±0.40	±0.22	±0.38

where X is defined through eq. (17) as

$$X = -\int_\Omega \varepsilon^{\mathrm{T}}(\beta,\gamma)\sin^2\beta\cos 2\gamma\,\mathrm{d}\Omega \Big/ \int_\Omega \varepsilon^{\mathrm{T}}(\beta,\gamma)\,\mathrm{d}\Omega. \quad (22)$$

For our trapezoidal detector, the "black" detector approximation at 3 cm gives for X a value of 0.03.

We have investigated the applicability of eq. (21) by measuring the directional correlation of the 570–1064 keV cascade in ^{207}Pb from a ^{207}Bi source. For this purpose the capability of a two-parameter analyzer was exploited. The two-parameter system has the great advantage that in one experiment one obtains two independent correlations for the same cascade of γ rays. In our case this allows for a double check of the Q values used. In fig. 7 we show a block diagram of the circuitry employed. Two charge sensitive, FET preamplifiers (Tennelec Model TC-135) and two Tennelec linear amplifiers (Model TC-200) were employed for linear pulse height analysis. Two base line restorers (Ortec Model 438) are used between the linear amplifiers and the pulse height analyzer when the singles rates exceed 3000 c/sec. It was found that optimum resolution could be achieved by using two delay line clipping amplifiers for cross-over timing, by employing the second output of the TC-135 preamplifiers. Two timing single channel analyzers were used and these were converted as shown to provide the coincidence output gate. A Cosmic Radiation Labs, Inc. multiple coincidence unit was employed for this purpose. The unit was modified to allow switching the fast coincidence requirement IN and OUT by means of dc levels set by the singles monitor control unit. This causes singles to be stored in the first plane of each axis for a preset fraction of the time. A time base generator (Cosmic Radiation Labs, Inc.) operated at 10 kC provided the clock pulses for driving a preset interval timer (Charter Laboratories Model 120). The time base generator can be blocked

TABLE 4
Estimated % errors in R_2 and R_4 due to extended sources, and off-axis positioning of the source.

Extended source			Source off-center		
Source radius (mm)	% error in R_2	% error in R_4	Distance off-center (mm)	% error in R_2	% error in R_4
0.5	−0.02	−0.04	0.5	−0.04	−0.08
1.0	−0.08	−0.16	1.0	−0.16	−0.32
2.0	−0.32	−0.64	2.0	−0.64	−1.28

when the buffer control unit is writing on magnetic tape. This allows one to maintain fixed singles to coincidence counting intervals.

The results from one typical angular correlation run of the 570–1064 keV cascade from ^{207}Bi are presented here. The two actual correlations measured from one two-parameter experiment can be represented by

$$W_{CT}(\theta) = A_{CT}[1 + A_{22}Q_2^C(570)Q_2^T(1064)F_2(\theta) + A_{44}Q_4^C(570)Q_4^T(1064)F_4(\theta)], \quad (23)$$

$$W_{TC}(\theta) = A_{TC}[1 + A_{22}Q_2^T(570)Q_2^C(1064)F_2(\theta) + A_{44}Q_4^T(570)Q_4^C(1064)F_4(\theta)], \quad (24)$$

where C refers to the 30 cm^3 Ge(Li) detector and T refers to the trapezoidal 20 cm^3 Ge(Li) detector. In table 5 we show the results of a typical measurement of $W_{CT}(\theta)$ and $W_{TC}(\theta)$, for distances of 3.0 and 4.0 cm from the trapezoidal and the cylindrical detectors, respectively. The data are normalized so that $W_{CT}(180°) = W_{TC}(180°) = 1.20$, thus facilitating a comparison between the two results. The last column in table 5 gives the combined average of the angular distribution. Fitting eqs. (23) and (24) to the data gives A_{CT} and A_{TC} which can be used to combine the two distributions $W_{CT}(\theta)$ and $W_{TC}(\theta)$ into one. The data in the last column in table 5 were fitted to the function

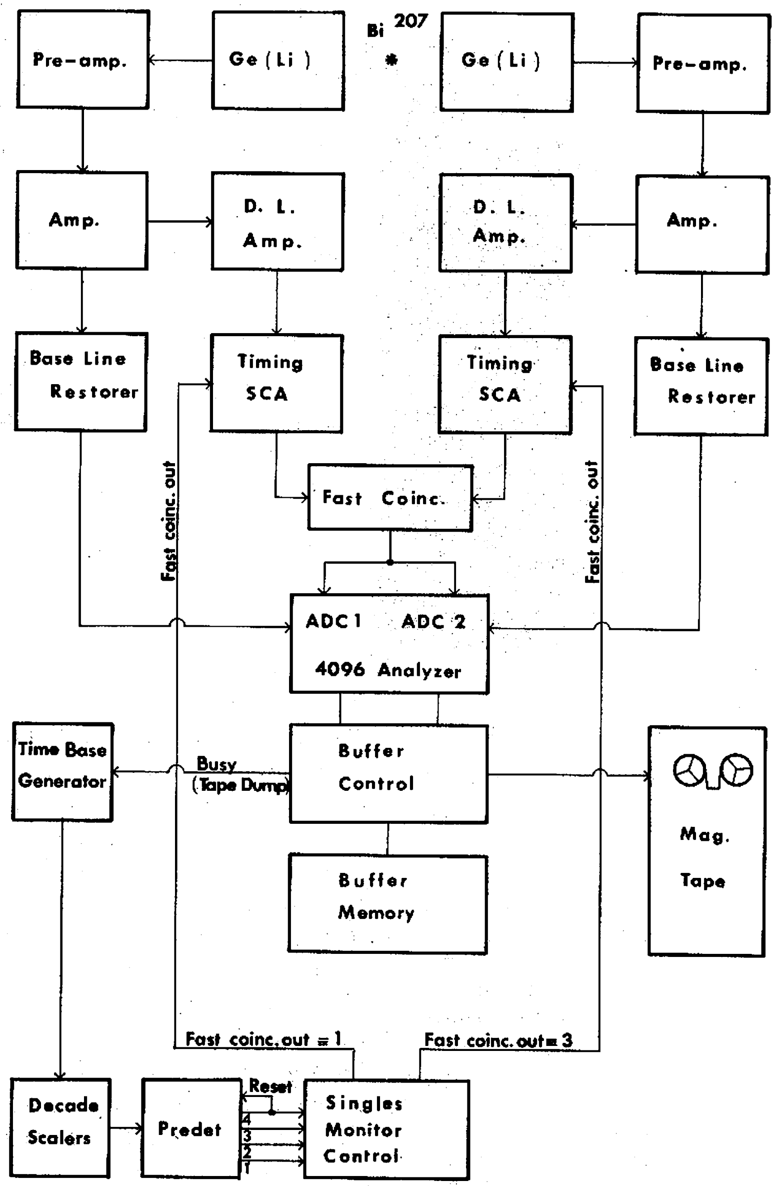

Fig. 7. Block diagram of the 2-parameter analyzer system employed in directional correlation measurements. The programming feature for monitoring the singles events in each Ge(Li) detector is also shown.

TABLE 5
Angular correlation data from the 570–1064 keV cascade in ^{207}Pb measured with two Ge(Li) detectors.

Angle	$W_{CT}(\theta)$	$W_{TC}(\theta)$	Combined average $W_{exp}(\theta)$
90°	0.915 ± 21	0.915 ± 19	0.915 ± 14
105°	0.953 ± 21	0.982 ± 24	0.968 ± 15
120°	1.033 ± 24	0.979 ± 21	1.006 ± 16
135°	1.132 ± 24	1.051 ± 23	1.091 ± 16
150°	1.146 ± 28	1.182 ± 24	1.164 ± 18
165°	1.176 ± 24	1.191 ± 23	1.184 ± 16
180°	1.200 ± 28	1.200 ± 24	1.200 ± 18

$$W_{exp}(\theta)/A = \tfrac{1}{2}[\{W_{CT}(\theta)/A_{CT}\}+\{W_{TC}(\theta)/A_{TC}\}], \quad (25)$$

which eliminates the constants A_{TC} and A_{CT} from expressions (23) and (24). Using the values of X equal to zero and 0.03 (estimate for a black detector) we obtain the results shown in table 6.

These results suggest that the largest A_{mm} coefficient of an angular correlation is rather insensitive to the value of X used; however, proper choice of X is more important in the determination of the smaller A_{mm} coefficient.

The above results are also in reasonable agreement with the previously reported values of A_{22} and A_{44} of 0.2180 ± 0.0043 and -0.0211 ± 0.0067 [3]) for this cascade, respectively. In fig. 8 we show the measured correlation. The solid line represents the best least-squares fit of $W_{exp}(\theta)/A$ to the data points with X equal to zero. The best curve fitted to the data with X equal to 0.030 was not clearly distinguished graphically from the curve shown in fig. 8, thus pointing out again the small dependence on X.

The data presented here were obtained under counting conditions anticipated for a typical case, where either half-life or source strength limitations determine the maximum rate of data accumulation. Thus, as an example, the value of $W_{CT}(\theta)$ (table 5) at 180° was obtained for a 4 hour counting period with a full energy peak count of approximately 2600 counts while the singles rate at the 1064 keV full-energy peak in the trapezoidal detector was 46 c/sec. The rate of random coincidences at the peak were only 3% of the coincidence plus randoms rate and thus corrections for this effect could be applied with confidence.

TABLE 6
Results of the analysis of the 570–1064 keV correlation in ^{207}Pb.

	$X=0$	$X=0.030$
A	1.0323 ± 58	1.0297 ± 55
A_{22}	0.226 ± 11	0.235 ± 12
A_{44}	−0.053 ± 22	−0.061 ± 25

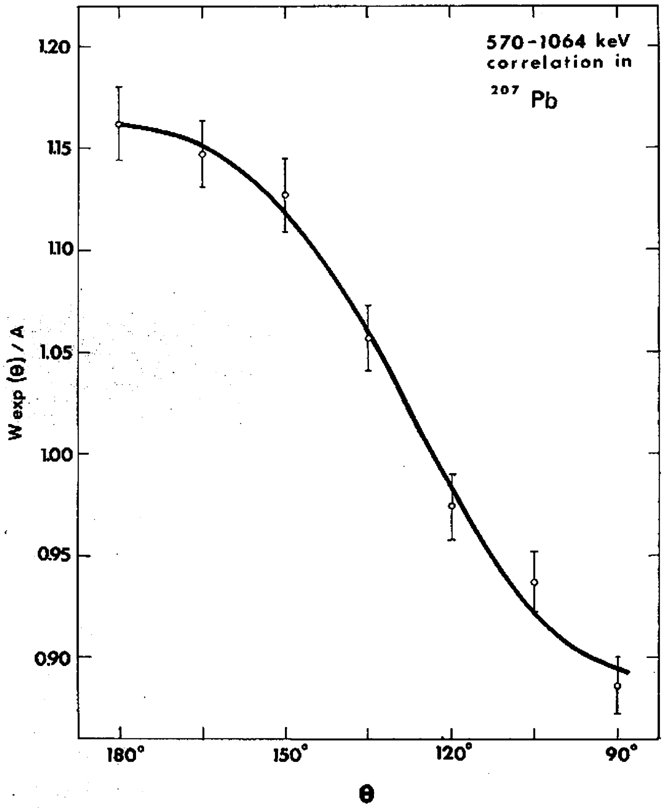

Fig. 8. Directional correlation of the 570–1064 keV cascade in ^{207}Pb measured with two Ge(Li) detectors and a two-parameter pulse height analyzer. The solid curve is the least-squares fit of expression (25) given in the text, to the data points.

In conclusion, we see that it is possible to measure reliable γ-γ angular correlations in nuclides emitting many γ rays by utilizing the high resolution of two large Ge(Li) detectors. As nuclides that emit many γ rays often populate many levels through different cascades, unique determination of the spins of such levels should evolve from this technique.

The authors are most grateful for the cooperation of Dr. T. Gallagher and the personnel of the Washington University Computing Facilities in processing these data. National Science Foundation Grant No. G-22296 is gratefully acknowledged.

The authors also wish to thank Mr. G. Kretschmann and Mr. P. Shocklee for the precise machining of the absorbers.

References

1) M. E. Rose, Phys. Rev. **91** (1953) 610.
2) M. J. L. Yates, Appendix 9 in *Alpha-, Beta- and Gamma-ray Spectroscopy* (ed. K. Siegbahn; North-Holland Publishing Company, Amsterdam, 1965).
3) F. K. McGowan and E. C. Campbell, Phys. Rev. **92** (1953) 523.